

Ultrahigh stability of atomically thin metallic glasses

C. R. Cao, K. Q. Huang, N. J. Zhao, Y. T. Sun, H. Y. Bai, L. Gu, D. N. Zheng, and W. H. Wang

Citation: [Applied Physics Letters](#) **105**, 011909 (2014); doi: 10.1063/1.4890113

View online: <http://dx.doi.org/10.1063/1.4890113>

View Table of Contents: <http://scitation.aip.org/content/aip/journal/apl/105/1?ver=pdfcov>

Published by the [AIP Publishing](#)

Articles you may be interested in

[Mechanical and thermal behaviors of nitrogen-doped Zr-Cu-Al-Ag-Ta—An alternative class of thin film metallic glass](#)

Appl. Phys. Lett. **101**, 181902 (2012); 10.1063/1.4759035

[Investigation on structural instability induced relaxation and crystallization in ZrCuAlNi bulk metallic glass](#)

J. Appl. Phys. **112**, 083530 (2012); 10.1063/1.4762013

[Mechanical behavior of a Zr-based metallic glass at elevated temperature under high strain rate](#)

J. Appl. Phys. **108**, 033511 (2010); 10.1063/1.3467779

[On the heating rate dependence of crystallization temperatures of metallic glasses](#)

J. Appl. Phys. **108**, 033515 (2010); 10.1063/1.3457336

[Influence of molten status on nanoquasicrystalline-forming Zr-based metallic glasses](#)

Appl. Phys. Lett. **93**, 261905 (2008); 10.1063/1.3046118



AIP | Journal of
Applied Physics

Journal of Applied Physics is pleased to
announce **André Anders** as its new Editor-in-Chief

Ultrahigh stability of atomically thin metallic glasses

C. R. Cao,^{a)} K. Q. Huang,^{a)} N. J. Zhao,^{a)} Y. T. Sun, H. Y. Bai, L. Gu,^{b)} D. N. Zheng,^{b)} and W. H. Wang^{b)}

Institute of Physics, Chinese Academy of Sciences, Beijing 100190, People's Republic of China

(Received 7 June 2014; accepted 30 June 2014; published online 10 July 2014)

We report the fabrication and study of thermal stability of atomically thin ZrCu-based metallic glass films. The ultrathin films exhibit striking dynamic properties, ultrahigh thermal stability, and unique crystallization behavior with discrete crystalline nanoparticles sizes. The mechanisms for the remarkable high stability and crystallization behaviors are attributed to the dewetting process of the ultrathin film. We demonstrated a promising avenue for understanding some fundamental issues such as glassy structure, crystallization, deformation, and glass formation through atomic resolution imaging of the two dimensional like metallic glasses. © 2014 AIP Publishing LLC.

[<http://dx.doi.org/10.1063/1.4890113>]

Metallic glasses (MGs) have a liquid-like atomic arrangement without long-range structural order.^{1–4} The atomic structure and their rearrangement play a key role in the basic properties such as glass-forming ability, crystallization, and deformations of MGs. Yet, the studies of their basic properties have been limited by the difficulty of directly observing the atomic structure and arrangements in glasses. As a result, the atomic-scale understanding of the fundamental phenomena such as crystallization, deformation, and relaxation have been conducted by computer simulation or pseudo-atomic systems such as micrometer scale colloidal particle. It is critical to develop or apply advanced experimental methods that can image atomic process of these phenomena with atomic resolution in glasses. So far, direct experimental access on the structure as well as its relationship with crystallization and properties in MG is very challenging.

Recently, it is found that the study of the atomic-scale thin non-metallic glassy films could shed light on some fundamental issues such as local structural characteristics, the thermodynamic and kinetic characteristics, and structural origins for relaxations, crystallization, and deformation of glasses.^{5–9} Benefited from modern technologies, the direct observation of atomic structure and dynamic processes down to sub-nanometer scale is now achievable,⁶ and the advancements might allow a direct assessment of atomic structures as well as their evolution during relaxations, crystallization, glass transition, and deformation in the MGs.¹⁰

In this paper, we report the formation of ultrathin glassy film (<1 nm in thickness, approach 2 dimensional MG). The crystallization behavior as well as its structural evolution, dynamic process was studied by a double spherical aberration-corrected high resolution scanning transmission electron microscope (Cs-STEM). The ultrathin film exhibits ultrahigh thermal stability and unique crystallization behavior. We show the ultrathin MG combining the atomic resolution microscopic method provide a promising avenue for understanding

long-standing fundamental issues on the structural characteristics, dynamic, and stability of glasses at atomic level.

The amorphous $Zr_{54}Cu_{38}Al_8$ films were deposited by pulsed laser deposition (PLD) in a high vacuum (10^{-6} Pa) chamber at room temperature. The substrate was electron-transparent TEM window grids (from SIMPORE, Inc.), which is a 5 nm thick amorphous silicon nitride ($a-Si_3N_4$) film support. Figure 1(a) illustrates the fabrication process of the glassy films by PLD. To ensure the uniformity of the thin film in composition, we used a glassy $Zr_{54}Cu_{38}Al_8$ PLD target, and the composition transfer congruence from the target alloy to the film in PLD was stable over a wide range of composition.¹¹ The depositing rate was ~ 0.03 nm/pulse calculated based on the results of X-ray reflectivity for several ultrathin films with different thickness (<5 nm).¹² The Cs-STEM [JEOL-ARM200F, with cold field-emission gun (CFEG)] and atomic force microscope (AFM) were used to characterize the structure and crystallization process of the films. The as-deposited films were *in situ* heated or annealed, and the substrate temperature was measured by a non-contact infrared thermometer. The annealed films were quickly transferred into Cs-STEM to avoid oxidation or pollution. No significant oxidation was found in the ultrathin film due to their glass nature with high resistance to oxidation.²

We used AFM to examine the uniformity of the ultrathin film. Figure 1(b) is the image of the $Zr_{54}Cu_{38}Al_8$ film with a thickness of about 0.3 nm deposited by PLD with 10 laser pulses on $a-Si_3N_4$ substrate. The similar random fluctuation morphology in the ultrathin film and the substrate demonstrates the randomly and homogeneously spread growth of the MG film on the $a-Si_3N_4$ substrate. The root-mean-square surface roughness (r) of the film and the $a-Si_3N_4$ substrate measured by AFM is about 0.232 ± 0.001 and 0.250 ± 0.001 nm, respectively. The substrate has slight wrinkling in three atomic size fluctuations, and the MG film has even smaller roughness indicating not an isolated islands growth mode like in thin crystalline film but a continuous thin layer growth mode.¹³ To further confirm its continuous growth mode, we compare the morphology of the MG films deposited on the surface of amorphous silicon oxide (1 nm in thickness) covering on monocrystalline silicon (with atomically flat surface smoothness of

^{a)}C. R. Cao, K. Q. Huang, and N. J. Zhao contributed equally to this work.

^{b)}Authors to whom correspondence should be addressed. Electronic addresses: l.gu@iphy.ac.cn; dzheng@iphy.ac.cn; and whw@iphy.ac.cn.

0.11 nm) and on the $a\text{-Si}_3\text{N}_4$ substrate. The r of the ultrathin MG film on the SiO_2 substrate is $\sim 0.067 \pm 0.001$ nm, which is smaller than one atomic size of 0.3 nm as the line profile shown in Fig. 1(c). This flatness is much close to the planar materials such as the graphene surface with a roughness in the

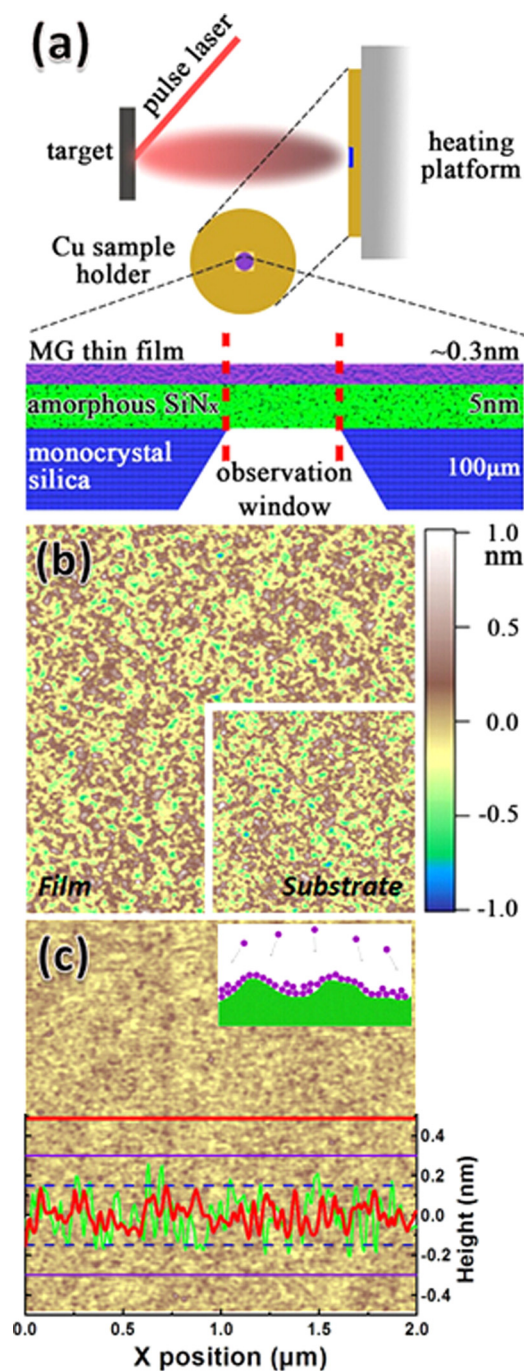


FIG. 1. (a) Schematic illustration of the deposition process of the PLD. The substrate was placed onto a Cu holder providing uniform heating field. The profile of ultrathin MG film deposited on the TEM window grids. (b) AFM images of surface topography of the film (scan range $2.0 \times 2.0 \mu\text{m}^2$) is similar to that of the $a\text{-Si}_3\text{N}_4$ substrate (bottom left inset image). (c) AFM images of as-grown film on SiO_2 substrate (scan range $2.0 \times 2.0 \mu\text{m}^2$) and the line profile of the atomically flatness surface of the ultrathin MG film (red serrated curve) is slight smoother than that of its substrate (green serrated curve). The thick purple line and thin blue line are the roughness limits within double and single atomic sizes. The top left inset shows the slight tendency of the depositing atoms flow into the low-lying areas indicating the liquid-like random growth mode.

order of 0.5 nm,^{14,15} which confirms that the ultrathin MG film on amorphous SiO_2 substrate is a continuous layer. Due to the fact that the surface energy¹⁶ and local lattice parameter¹⁷ of amorphous SiO_2 and $a\text{-Si}_3\text{N}_4$ substrates are similar, the MG film should have similar growth mode on the two substrates, and the decrease of the roughness after film deposition indicates that there are no terrace or island boundaries on the substrates. AFM results further confirm that the ultrathin MG film on the $a\text{-Si}_3\text{N}_4$ is in a continuous layer growth mode, and likes a 2D liquid layer covering on the plicate surface as illustrated in the inset of Fig. 1(c).

Figure 2(a) is the high-angle annular-dark-field (ADF) image of $\text{Zr}_{54}\text{Cu}_{38}\text{Al}_8$ film on $a\text{-Si}_3\text{N}_4$ with $40 \times 65 \text{ nm}^2$ scan range. The 0.3 nm thin film flat covers on the substrate, and the enlarge picture in Fig. 2(b) shows that the atoms distributed randomly on the substrate. Benefited from the atomic-resolution image, we identify that the most of the bright spots in this image represent Zr atoms although there are few stacks of metallic atoms appear as an intensity inhomogeneous distribution. The density of the MG film then can be estimated from the bright spots in the TEM images, and the obtained total atomic density is about $13.01 \pm 3 \text{ atoms nm}^{-2}$, which is comparable to that of a 2D SiO_2 glass.¹⁸ We also deposited pure Cu on $a\text{-Si}_3\text{N}_4$ with the same conditions. In contrast, the Cu ultrathin film grew obvious into paracrystal 3D islands with a low density and there are few metallic atoms around the particle [see Fig. 2(c)], which is totally different from the growth mode of MG film. The Cs-STEM results also confirm that the ultrathin MG film is a continuous layer of atoms on the plicate surface.

The glass transition temperature T_g^{bulk} , crystallization temperature T_x^{bulk} , melting temperature T_m^{bulk} , and liquidus temperature T_l^{bulk} of bulk $\text{Zr}_{54}\text{Cu}_{38}\text{Al}_8$ MG (Ref. 19) are 680, 757, 1056, and 1156 K, respectively. Annealing or heating close to T_x leads to rapid crystallization for conventional MGs.⁸ Figure 3(a) presents Cs-STEM ADF image of the MG ultrathin films annealed at $873 \pm 15 \text{ K}$ for about 20 min, which is 100 K above T_x^{bulk} . Remarkably, the annealed

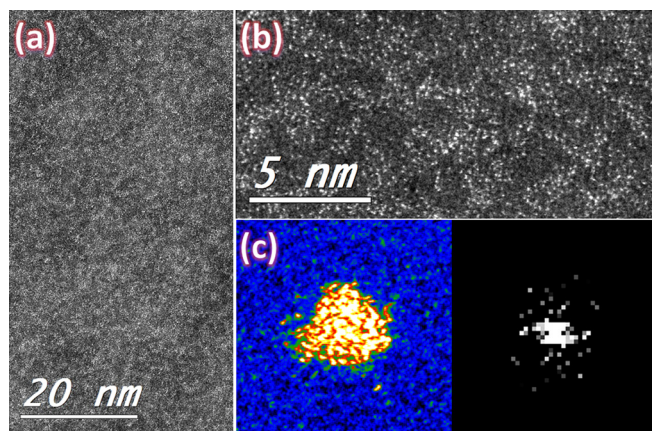


FIG. 2. Cs-STEM dark-field images of the distribution of metallic atoms in the ultrathin film. (a) The atomic resolution Cs-STEM image of the 0.3 nm thin MG film with $40 \times 65 \text{ nm}^2$ scan range, and the clear random distribution of metallic atoms (bright spots); (b) The enlarge Cs-STEM image of (a); (c) The Cs-STEM image ($5 \times 5 \text{ nm}^2$ scan range) of as-grown Cu paracrystal grain nucleation on $a\text{-Si}_3\text{N}_4$, and the right image is the FFT of Cu paracrystal grain.

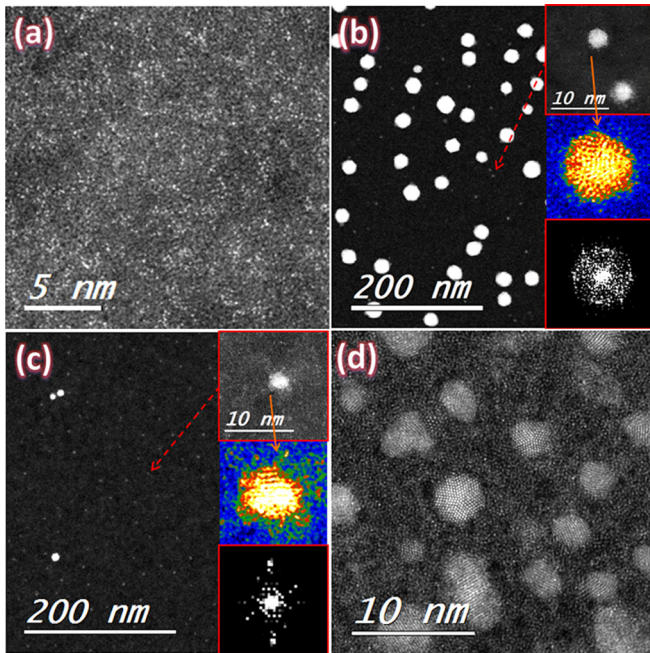


FIG. 3. Cs-STEM dark-field images of annealed MG thin films with different thickness. (a) The 0.3 nm MG film annealed at 873 ± 15 K for 20 min. (b) The image (micron-sized scan range) of the 0.3 nm MG film heated to 1056 ± 15 K. (c) 0.7 nm MG film heated to 873 ± 15 K. The top left of images (b) and (c) are the zoom-in images of the regions around the smaller paracrystal grains of the two samples, their enlarged colored images, and local FFTs showing the symmetry structure of the grains. (d) 3 nm thickness film crystallized at 873 ± 15 K showing higher density and ordered structures of crystal grains.

glassy film shows no sign of nucleation and formation of crystalline phase indicating the thermodynamically ultrastable nature of the MG film compared to that of its bulk form.

To understand the high thermal stability of the film, we investigated the crystallization behavior of the film and heated the sample *in situ* at 1053 ± 15 K (near T_i^{bulk} of 1056 ± 5 K). Figure 3(b) is the Cs-STEM images of the heated MG film. The crystallization behavior of the ultrastable MG film is totally different from that of conventional MGs. There are a number of hexagon crystalline particles embedded in the glassy matrix with almost the same size of 25 nm, and around these hexagon particles there are higher density crystalline circular particles with almost same diameter of 3 nm. This unique crystallization with two types of discrete crystalline nano-particles sizes has not been reported in crystallization of bulk MGs, which always has a wide range of crystalline size distribution.²⁰ The crystallization behavior and thermal stability of the MG films depend on their thickness, and their thermal stability decreases with the increase of their thickness. The MG film in thickness of 0.7 nm heated to 873 ± 15 K also shows the two types of quantized grain sizes [see Fig. 3(c)], in contrast to that in 0.3 nm film heated at 1053 ± 15 K [Fig. 3(b)], there are plentiful atoms around the smaller paracrystal grains. The insets in Figs. 3(b) and 3(c) are, respectively, the enlarged and local fast Fourier transform (FFT) images of the smaller paracrystal particles, which show that the small particles have structural symmetry even though they are not fully crystalline phase. In contrast, the crystallization of thick MG film (3 nm in thickness,

annealed at 873 K for 20 min) shows no obvious discrete grain sizes but higher density various irregular crystalline grains in amorphous matrix [Fig. 3(d)].

We note that the discrete crystallized grains phenomenon has also been observed in the single substance systems, which is attributed to the dewetting process²¹ and in bulk MGs which is attributed to the spinodal decomposition or the larger diffusion barriers.^{22,23} In thin gold film, the quantized sizes feature resulting from the dewetting appeared only when its thickness is larger than 5 nm accompanying with a long time annealing near melting temperature. This indicates that the crystallization mechanism in the ultrathin MG films could be similar to that of the simple substance systems due to their similar crystallization behaviors. To investigate the dynamic behavior of the crystallization of the ultrathin MG film, we used the electron beam to irradiate the 0.3 nm MG film. In the center 5×5 nm area of Fig. 4(a), the film was irradiated with an illumination dose rate of $\sim 1.7 \times 10^6$ electrons/nm²s and frame rates of ~ 0.5 s (200 kV) lasted for ~ 8 min. The electrons transferred sufficient local energy to eject atoms and even result in the perforation in the a-Si₃N₄ substrate. Comparing with Fig. 4(b), we see that the MG film around the high dose irradiated area shows obvious tendency of atoms self-assembly through the dewetting process²⁴ in Fig. 4(c). The dewetting phenomenon of the MG film, which has also been reported in various other thin film systems,^{24,25} is a high surface tension impelled atoms process when the atoms in the film was activated. It is the dewetting process that induces the crystallization behavior.²⁶

In glassy thin films, the prerequisites for dewetting process include: temperature T must be above T_g of the film for the atoms can flow and self-aggregate above T_g ;²⁷ the

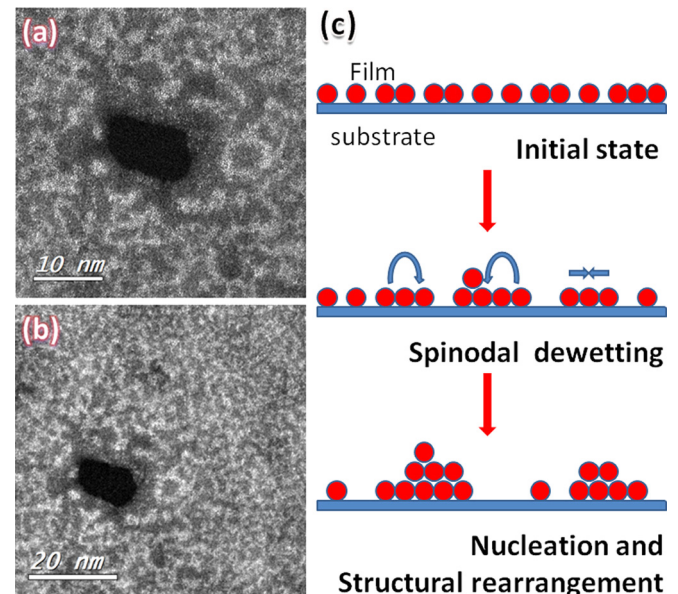


FIG. 4. (a) The Cs-STEM dark-field images of *in situ* electron beam irradiation induced perforation, and the metallic atoms self-aggregate around the hole. (b) Larger view of the region in (a); the obvious tendency of the metallic atoms self-aggregate near the hole around can be seen along the heat transfer direction. (c) Schematic illustration of the nucleation process, atomic rearrangement and formation of small 3D islands of the ultrathin film (< 1 nm). In initial state, the atoms flat on the substrate; as $T > T_g$, the atoms begin to self-aggregate as the spontaneous dewetting process supported by high atomic density around the islands at a high T .

substrate surface has to be non-wettable for the film; and the negative spreading coefficient $S = \gamma_s - \gamma_{fs} - \gamma_f < 0$,²⁸ where γ_s , γ_{fs} , and γ_f are the substrate surface energy, the film/substrate interfacial energy, and film surface energy, respectively. Although in an ultrathin film system γ_f and γ_{fs} depend on its thickness, the film could prefer to take lattice strain from the lattice mismatch at the film/substrate interface to avoid the formation of non-coherent interface with a larger γ_{fs} and lower γ_f and to minimize the total free energy of the film.²⁹ The γ_f of this MG film can be roughly regarded to be the surface tension of the melting bulk Zr-based MGs ($\sim 1.5 \text{ J/m}^2$ (Ref. 30)) and γ_s of a-Si₃N₄ is less than 1 J/m^2 .¹⁶ Therefore, the interaction between the film and substrate is $\gamma_{fs} > \gamma_s - \gamma_f > -0.5 \text{ J/m}^2$, which is weak enough for the happening of the spontaneous dewetting process during annealing in the MG film. The spontaneous dewetting as a result provides favorable conditions for the 3D nucleation process as indicated in Fig. 4(c). The Cs-STEM images in Fig. 3 indicate that the crystallization products of the MG film are 3D particles instead of a monolayer hexagonal lattice structure like graphene. The formation of the 3D crystalline phases is the requirement of the ultrathin film crystallization, and the nucleation and growth of the 3D crystalline phases need to overcome the large kinetic barriers from the interaction between the film and substrate, and the long-range atomic diffusion barrier.³¹ This is the main reason for the highly stable behavior of the ultrathin MG film.

The high thermal stability is also related to the thickness h of the film due to the fact that island nucleation rate n on a surface is:³² $n \sim D(\rho h)^2$. Here, D is the diffusion constant and ρ is the surface atomic density of the film. Therefore, the thicker MG film with higher atomic density area induced by the dewetting process has the favorable conditions for nucleation, in agreement with our observations of the thermal stability of the MG films decreases with the increase of their thickness. From the energy landscape perspective, the ultrafast surface dynamics of the ultrathin MG system could relax the several atomic layers of the glass surface into a lower energy minima, and leads to the increase of the thermal stability,^{33,34} which has also been observed on the surface of Ce-base MGs (Ref. 33) and various glass films.^{5,8,34} From thermodynamic point of view, the melting temperature T_m of an ideal infinitely large crystal films can be expressed as:³⁵ $T_m = T_m^{\text{bulk}} (1 - \frac{2\gamma_f}{\rho h \Delta H_f})$, where ΔH_f is the enthalpy of fusion. The T_m decreases with the decrease of the thickness of the film. In a finite size, the T_m suppression would slow crystallization kinetics due to the thermodynamic destabilization of the crystal relative to the supercooled liquid, i.e., there is a decrease in the effective undercooling at a given temperature. This would also result in a higher crystallization temperature of the MG film.³⁶

The random disordered network structure of the a-Si₃N₄ substrate with high thermal stability cannot provide the heterogeneous crystallization nucleation sites for the crystallization of the MG film, and the crystallization of the MG film and even pure Cu film can avoid heterogamous nucleation,³⁷ as shown in Fig. 2(c). The Cu, Al, especially Zr atoms have high negative mixing enthalpy with Si atom in substrate indicating the bonding effect between the MG film and the substrate. The crystallization of the film is controlled by the

dynamic of the atoms especially the Zr atoms, as shown in Figs. 3 and 4. The binding effects and the homogeneous nucleation limit the kinetics of atoms especially of Zr in the MG film, and then inhibit the crystallization and enhance the thermal stability of the MG films.

In conclusions, the atomically thin MG film exhibits remarkable high thermal stability and unique crystallization behavior relative to its bulk form. The results shed light on the dynamic characteristics and atomic mechanism of crystallization and formation, as well as the shear banding behavior which is regarded as a thin liquid like layer of metallic glasses, and would have practical implications for thin-film coatings related to lubrication, wear, and friction. The atomically thin MG film combining the Cs-STEM techniques with well-defined *in situ* stimuli such as heating and straining are desirable to study local structural features and dynamic processes in the glassy materials at atomic level.

The insightful discussions and experimental assistance from D. Q. Zhao, D. W. Ding, M. X. Pan, M. Gao, B. A. Sun, S. M. Li, and J. A. Shi are appreciated. This work was supported by the NSF of China (Grant No: 51271195) and MOST 973 (No. 2014CB921002).

¹D. B. Miracle, *Nat. Mater.* **3**, 697 (2004).

²D. Ma, A. D. Stoica, and X.-L. Wang, *Nat. Mater.* **8**, 30 (2009).

³M. Leocmach and H. Tanaka, *Nat. Commun.* **3**, 974 (2012).

⁴V. Borodin, *Philos. Mag. A* **79**, 1887 (1999).

⁵S. F. Swallen, K. L. Kearns, M. K. Mapes, Y. S. Kim, R. J. McMahon, M. D. Ediger, T. Wu, L. Yu, and S. Satija, *Science* **315**, 353 (2007).

⁶P. Y. Huang, S. Kurasch, J. S. Alden, A. Shekhawat, A. A. Alemi, P. L. McEuen, J. P. Sethna, U. Kaiser, and D. A. Muller, *Science* **342**, 224 (2013).

⁷M. Tress, E. U. Mapesa, W. Kossack, W. K. Kipnusu, M. Reiche, and F. Kremer, *Science* **341**, 1371 (2013).

⁸H. B. Yu, Y. Luo, and K. Samwer, *Adv. Mater.* **25**, 5904 (2013).

⁹D. P. Aji and M. W. Chen, preprint [arXiv:1306.1575](https://arxiv.org/abs/1306.1575) (2013).

¹⁰M. Heyde, *Science* **342**, 201 (2013).

¹¹C. B. Arnold and M. J. Aziz, *Appl. Phys. A* **69**, S23 (1999).

¹²R. Lazzari, G. Renaud, J. Jupille, and F. Leroy, *Phys. Rev. B* **76**, 125412 (2007).

¹³J. Venables, *Introduction to Surface and Thin Film Processes* (Cambridge University Press, 2000).

¹⁴C. Lee, Q. Li, W. Kalb, X.-Z. Liu, H. Berger, R. W. Carpick, and J. Hone, *Science* **328**, 76 (2010).

¹⁵S. S. Datta, D. R. Strachan, S. M. Khamis, and A. C. Johnson, *Nano Lett.* **8**, 1912 (2008).

¹⁶S. Sanchez, C. Gui, and M. Elwenspoek, *J. Micromech. Microeng.* **7**, 111 (1997).

¹⁷W. O'Mara, R. B. Herring, and L. P. Hunt, *Handbook of Semiconductor Silicon Technology* (Crest Publishing House, 2007).

¹⁸L. Lichtenstein, C. Büchner, J. Sauer, and H. J. Freund, *Angew. Chem. Int. Ed.* **51**, 404 (2012).

¹⁹D. Wang, H. Tan, and Y. Li, *Acta Mater.* **53**, 2969 (2005).

²⁰W. H. Wang, C. Dong, and C. H. Shek, *Mater. Sci. Eng., R* **44**, 45 (2004).

²¹C. M. Müller, F. C. F. Mornaghini, and R. Spolenak, *Nanotechnology* **19**, 485306 (2008).

²²K. Kelton, T. Croat, A. Gangopadhyay, L.-Q. Xing, A. Greer, M. Weyland, X. Li, and K. Rajan, *J. Non-Cryst. Solids* **317**, 71 (2003).

²³S. Bhattacharyya, C. Bocker, T. Heil, J. r. R. Jinschek, T. Höche, C. Rüssel, and H. Kohl, *Nano Lett.* **9**, 2493 (2009).

²⁴S. Herminghaus, K. Jacobs, K. Mecke, J. Bischof, and S. Schlagowski, *Science* **282**, 916 (1998).

²⁵J. Becker, G. Grün, R. Seemann, K. R. Mecke, and R. Blossey, *Nat. Mater.* **2**, 59 (2003).

²⁶H. S. Kheshti and L. Scriven, *Chem. Eng. Sci.* **46**, 519 (1991).

²⁷I. Karapanagiotis and W. W. Gerberich, *Surf. Sci.* **594**, 192 (2005).

²⁸P.-G. De Gennes, *Rev. Mod. Phys.* **57**, 827 (1985).

- ²⁹S. Burke, J. Topple, and P. Grütter, *J. Phys.: Condens. Matter* **21**, 423101 (2009).
- ³⁰S. Mukherjee, W. Johnson, and W. Rhim, *Appl. Phys. Lett.* **86**, 014104 (2005).
- ³¹G. Reiter, A. Sharma, A. Casoli, R. Khanna, and P. Auroy, *Langmuir* **15**, 2551 (1999).
- ³²J. Tersoff, A. D. Van der Gon, and R. Tromp, *Phys. Rev. Lett.* **72**, 266 (1994).
- ³³S. Ashtekar, D. Nguyen, W. H. Wang, and M. Gruebele, *J. Chem. Phys.* **137**, 141102 (2012).
- ³⁴Y. Guo, A. Morozov, D. Schneider, J. W. Chung, C. Zhang, M. Waldmann, N. Yao, G. Fytas, C. B. Arnold, and R. D. Priestley, *Nat. Mater.* **11**, 337 (2012).
- ³⁵Y. Wang, S. Ge, M. Rafailovich, J. Sokolov, Y. Zou, H. Ade, J. Lüning, A. Lustiger, and G. Maron, *Macromolecules* **37**, 3319 (2004).
- ³⁶M. Gopinadhan, Z. Shao, Y. Liu, S. Mukherjee, R. C. Sekol, G. Kumar, A. D. Taylor, J. Schroers, and C. O. Osuji, *Appl. Phys. Lett.* **103**, 111912 (2013).
- ³⁷Q. An, S.-N. Luo, W. A. Goddard, and W. L. Johnson, *Appl. Phys. Lett.* **100**, 041909 (2012).